Bone 66 (2014) 306–314

Contents lists available at ScienceDirect

Bone

journal homepage: www.elsevier.com/locate/bone

Original Full Length Article

Ginsenoside-Rb_2 displays anti-osteoporosis effects through reducing oxidative damage and bone-resorbing cytokines during osteogenesis

Qiang Huang [1], Bo Gao [1], Qiang Jie [1], Bo-Yuan Wei, Jing Fan, Hong-Yang Zhang, Jin-Kang Zhang, Xiao-Jie Li, Jun Shi, Zhuo-Jing Luo [2], Liu Yang [2], Jian Liu *

Institute of Orthopedic Surgery, Xijing Hospital, Fourth Military Medical University, Xi'an 710032, People's Republic of China

ARTICLE INFO

Article history:
Received 27 February 2014
Revised 5 June 2014
Accepted 6 June 2014
Available online 13 June 2014

Edited by J. Aubin

Keywords:
Ginsenoside-Rb_2
Oxidative damage
Osteogenesis
Osteoporosis
Ovariectomized mouse
Bone-resorbing cytokine

ABSTRACT

Reactive oxygen species (ROS) are a significant pathogenic factor of osteoporosis. Ginsenoside-Rb_2 (Rb_2), a 20(S)-protopanaxadiol glycoside extracted from ginseng, is a potent antioxidant that generates interest regarding the bone metabolism area. We tested the potential anti-osteoporosis effects of Rb_2 and its underlying mechanism in this study. We produced an oxidative damage model induced by hydrogen peroxide (H_2O_2) in osteoblastic MC3T3-E1 cells to test the essential anti-osteoporosis effects of Rb_2 *in vitro*. The results indicated that treatment of 0.1 to 10 μM Rb_2 promoted the proliferation of MC3T3-E1 cells, improved alkaline phosphatase (ALP) expression, elevated calcium mineralization and mRNA expressions of *Alp*, *Col1a1*, *osteocalcin* (*Ocn*) and *osteopontin* (*Opn*) against oxidative damage induced by H_2O_2. Importantly, Rb_2 reduced the expression levels of receptor activator of nuclear factor kappa-B ligand (RANKL) and IL-6 and inhibited the H_2O_2-induced production of ROS. The *in vivo* study indicated that the Rb_2 administered for 12 weeks partially decreased blood malondialdehyde (MDA) activity and elevated the activity of reduced glutathione (GSH) in ovariectomized (OVX) mice. Moreover, Rb_2 improved the micro-architecture of trabecular bones and increased bone mineral density (BMD) of the 4th lumbar vertebrae (L4) and the distal femur. Altogether, these results demonstrated that the potential anti-osteoporosis effects of Rb_2 were linked to a reduction of oxidative damage and bone-resorbing cytokines, which suggests that Rb_2 might be effective in preventing and alleviating osteoporosis.

Introduction

Oxidative stress is described as an imbalance between an overproduction of reactive oxygen species (ROS) and an insufficient defense of antioxidants [1]. Oxidative stress can lead to oxidative damage that affects all of the cellular components, including proteins, lipids and nucleic acids. Osteoporosis is defined as a systemic degenerative disease, which is characterized by decreased bone mass and progressive bone micro-architectural deterioration and results in increasing bone fragility and susceptibility to fractures [2]. Currently, many studies have demonstrated a relationship between oxidative damage and osteoporosis or aging. Sendur and colleagues found that the decreased BMD of postmenopausal osteoporotic women was related to higher oxidation of plasma lipid [3] and lowered superoxide dismutase (SOD), catalase and glutathione peroxidase efficacy [4–6]. Ovariectomy has been shown to induce oxidative damage and to decrease the efficacy of antioxidant defense mechanisms, thus leading to osteoporosis. The activities of lipid peroxidation and H_2O_2 were increased, and enzymatic antioxidants, such as superoxide dismutase, glutathione peroxidase, and glutathione S transferase, were decreased in ovariectomized animals [7]. Moreover, many studies have demonstrated that superoxide and H_2O_2 were highly deleterious to cell survival and that they played a major causative role in the aging process [8]. These research findings provided a paradigm shift of osteoporosis pathogenesis from the "estrogen-centric" concept to one in which age-related mechanisms intrinsic to bone and oxidative stress were protagonists. Moreover, the age-related changes in other organs and tissues, such as the ovaries, accentuated these alterations [9].

Bone remodeling is a process that occurs throughout one's entire life and involves two types of cells: osteogenic cells and monocyte-derived osteoclasts [10–12]. The osteogenic cells participate in bone formation, and osteoclasts are responsible for bone resorption [13,14]. The balance between bone formation and bone resorption is essential for maintaining bone homeostasis. Bone turnover changes significantly in postmenopausal osteoporosis: bone resorption is maintained or increases, but bone formation decreases, thereby leading to a net bone loss [15].

Emerging evidence has shown that ROS increased bone resorption by enhancing osteoclastic development and activity [16]. Indeed, *in vivo* bone resorption occurs preferentially in sites where ROS and

* Corresponding author. Fax: +86 29 84771013.
E-mail address: liujianhq@sina.com (J. Liu).
[1] These authors contributed equally to the work.
[2] Co-corresponding author.

http://dx.doi.org/10.1016/j.bone.2014.06.010

hence oxidative stress levels are high [17,18]. ROS also led to osteoblast apoptosis, as well as reducing their activity, which led to decreased osteogenesis [19]. Oxidative stress decreases the life span of osteoblast in the bone, as highlighted by the observation that the administration of antioxidants abrogates osteoblast apoptosis in ovariectomized or aged mice [20,21]. Therefore, we recommend substances that contain antioxidants because they may ameliorate the dysfunction of these two cell types by maintaining bone hemostasis. This suggestion might be implemented by acting as a latent method for the prevention and new treatment for osteoporosis or other related bone metabolic diseases.

Because of fewer side-effects and longer term usage than Western medicine, traditional Chinese medicines with anti-oxidative properties have recently attracted more attention. The ginseng root, which is a highly effective phyto medicinal remedy, is a well-recognized, traditional Chinese medicine that is widely used. The primary components found in ginseng are ginsenosides, which contribute to the most active properties. Ginsenoside-Rb_2 (Fig. 1) is the most quantitative saponin that is contained in *Panax ginseng* [22]. It was reported that Rb_2 possessed anti-diabetic, anti-adipocyte, anti-carcinogenic and anti-oxidative properties [23–26]. More importantly, recent studies showed that H_2O_2, which is known as a cancer promoter, inhibited the gap junctional intercellular communication (GJIC) of epithelial cells. Rb_2 supplementation might inhibit the occurrence of cancer through the up-regulation of GJIC in the cancer-accelerating phase [27]. SOD1 is considered to be one of the antioxidant enzymes. A previous study [28] has shown that ginsenoside-Rb_2 could induce the transcriptional expressions of *Cu, Zn-superoxide dismutase* gene (*SOD1*). The mutated AP2 binding site in the promoter of *SOD1* gene abrogated this effect, which suggests that the *SOD1* gene was highly activated by ginsenoside-Rb_2 through the AP2 binding site [28]. Kang et al. studied the hydroxyl radical (•OH) clearing capacity change of Rb_2 through heat procedure using an electron spin resonance spectrometer. Specially, ginsenoside-Rb_2 was heat processed using the same amount of glycine, which was an amino acid commonly employed in the Maillard response model system [26].

Whether ginsenoside-Rb_2 might provide the potential anti-osteoporosis effects and whether these effects are produced by reducing oxidative damage and bone-resorbing cytokines have not been established. Therefore, in the present study, we tested the anti-osteoporosis effects of Rb_2 and the underlying mechanisms *in vitro* and *in vivo* using an H_2O_2-induced oxidative damage model of osteoblastic MC3T3-E1 cells and a murine ovariectomized model.

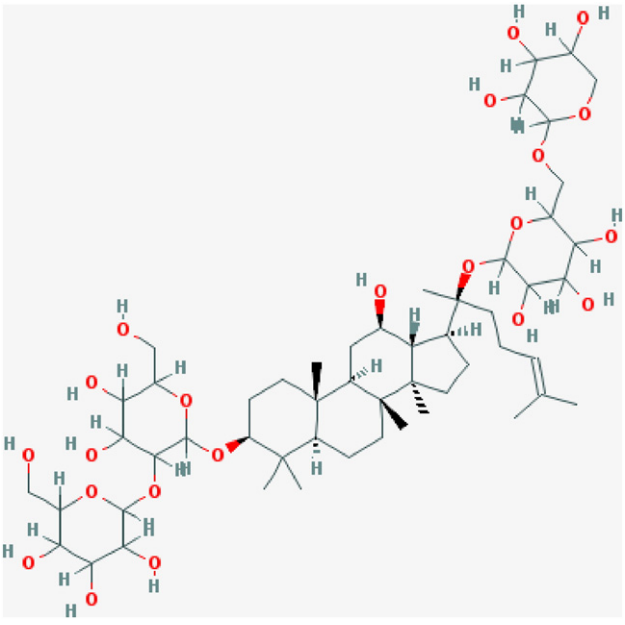

Fig. 1. Chemical structure of Rb_2 (from National Center of Biotechnology Information, Pubchem CID: 5458674).

Materials and methods

Materials

Rb_2 extracted from ginseng (molecular weight, 1079; purity, >98.0%; dissolved in distilled water) was purchased from Shanghai Tauto Biotech Co., LTD (China). The culture flasks and plates were obtained from Nunc (Denmark). The ALP activity assay kit was obtained from GENMED Scientific Inc. (USA). RANKL and IL-6 ELISA assay kits were obtained from R&D system Inc. (Minneapolis, MN, USA). The total RNA kit was obtained from OMEGA. Prime Script RT reagent kit and SYBR Premix Ex Taq were obtained from TaKaRa Biotechnology (Dalian, China). The oligonucleotide primers were synthesized by TaKaRa Biotechnology. BCIP/NBT alkaline phosphatase color development kit was obtained from Gibco Life Technologies (Grand Island, USA). The reactive oxygen species assay kit, GSH and MDA assay kits were obtained from the Beyotime Institute of Biotechnology (Shanghai, China). All other reagents were of analytical grade.

Cell cultures

Murine MC3T3-E1 cells were purchased from the Center Laboratory for Tissue Engineering, College of Stomatology, Fourth Military Medical University, Xi'an, China [29,30]. The cells were cultured in α-MEM using 10% heat-inactivated FBS and 100 U/ml penicillin and 100 mg/ml streptomycin in a condition of 5% CO_2 and 37 °C. H_2O_2 acted as exogenous ROS treatment, whereas N-acetyl-L-cysteine (NAC) acted as an ROS cleaner. When the cells reached confluence, the serum-free medium containing Rb_2 was dissolved in distilled water and cultured for 24 h before the administration of 0.3 mM H_2O_2 for 24 h. For each experiment, Rb_2 administration continued after the pretreatment. All of the experiments were performed in duplicate wells and repeated three times.

Assays of cell survival

For this experiment, the murine MC3T3-E1 cells were administered using different consistencies of Rb_2 (0 μM, 0.1 μM, 1 μM, and 10 μM) for 24 h and 72 h to test the toxicity of Rb_2. Subsequently, the cells were incubated using the serum-free regular culture medium, which contained Rb_2 (0 μM, 0.1 μM, 1 μM, and 10 μM) for 24 h followed by the administration of 300 μM H_2O_2 for 24 h. The MTT assays were used for measuring cell survival. The absorbances of all of the wells were recorded using a micro-plate reader at 492 nm wavelength. The cell survival of the control group, which was not exposed to either H_2O_2 or Rb_2, was defined as 100%.

Alkaline phosphatase (ALP) staining and activity assay

After a 6-day osteogenic induction, the murine MC3T3-E1 cells were incubated using serum-free medium, which contained Rb_2 and/or H_2O_2 for 2 days. The cells were stained using the BCIP/NBT alkaline phosphatase color development kit according to the manufacturer's instructions. To evaluate the ALP activity, the cell monolayer was lysed using the cell lysis buffer. Subsequently, the lysate was centrifuged at 10,000 *g* for 5 min. The clear supernatant was used to measure the ALP activity, which was determined employing the ALP activity assay kit. The total protein consistencies were determined using the Bradford protein assay method. The ALP activity was normalized to total protein, which was measured using the Bradford protein assay method.

Calcium mineralization assay

After a 21-day osteogenic induction, the murine MC3T3-E1 cells were incubated using a serum-free medium, which contained Rb_2

and/or H_2O_2 for 2 days. After the cells were collected, the cells were fixed with formalin for 20 min and stained with Alizarin Red S for 45 min under room temperature. To measure matrix calcification, unbound alizarin red was washed off using PBS. Subsequently, the stain was solubilized using 10% cetylpyridinium chloride by shaking for 15 min. The absorbances of the released Alizarin Red S were recorded using a micro-plate reader at 562 nm wavelength.

Quantitative real-time PCR

After a 6-day osteogenic induction, murine MC3T3-E1 cells were incubated using a serum-free medium, which contained Rb_2 and/or H_2O_2 for 2 days. The total cellular RNA was extracted from these cells using Trizol reagent. Single strand cDNA synthesis was determined using the Prime Script RT reagent kit (TaKaRa). The RT-PCR was performed using the CFX96 (BIO-RAD) instrument, and individual PCRs were conducted in 96-well optical reaction plates using SYBR Green-I (TaKaRa) according to the manufacturer's instructions. Target gene (*Alp*, *Col1a1*, *Ocn* and *Opn*) expressions were normalized to the reference gene *β-actin*. The $2^{-\Delta\Delta Ct}$ method was applied to calculate the relative gene expression. These PCR products were subjected to a melting curve analysis and a standard curve to confirm the correct amplification. All of the PCRs were performed in triplicate, and the primers used for PCR are shown in Table 1.

RANKL and IL-6 measurements

After a 6-day osteogenic induction, the murine MC3T3-E1 cells were incubated using serum-free medium, which contained Rb_2 and/or H_2O_2 for 2 days. The expressions of RANKL and IL-6 in culture medium were tested using the sandwich ELISA assay kit according to the manufacturer's instructions. The total protein consistencies were measured using the Bradford protein assay method.

Intracellular reactive oxygen species (ROS) measurement

After a 6-day osteogenic induction, the murine MC3T3-E1 cells were incubated using serum-free medium, which contained Rb_2 and/or H_2O_2 for 2 days. The intracellular ROS expression level was determined using the ROS assay kit. DCFH-DA can be oxidized by ROS in viable cells to 2′,7′-dichlorofluorescein (DCF), which is highly fluorescent at 530 nm. These cells were washed three times with PBS. DCFH-DA, which was diluted to a final consistency of 10 μM, was added and cultured for 30 min at 37 °C in the dark. When washed three times by PBS, the relative expression of fluorescence was quantified using a multi-detection micro-plate reader (485 nm excitation and 535 nm emission).

Animals and ginsenoside-Rb_2 intervention

Forty 8-week-old, BALB/c female mice, weighing 20.84 ± 1.21 g, were obtained from the Experimental Animal Center of The Fourth Military Medical University (Xi'an, China). There was no significant difference in the initial body weights of the mice among all 4 groups in this experiment. The mice were allowed to adapt to the laboratory environment (a well-ventilated controlled room at 20 °C on a 12-h light/dark cycle; the animals were given free access to water and food) for 1 week before the surgery. Subsequently, the mice experienced sham-operation (n = 10) or were surgically ovariectomized (OVX) (n = 30) under anesthesia using pentobarbital sodium (50 mg/kg body weight, i.p.). The ovariectomy operation was performed according to Steven K. Boyd's procedure [31]. A total of 30 BALB/c female mice were randomly divided into three groups: 1) OVX group, administered intraperitoneally with distilled water (n = 10); 2) OVX group, administered intraperitoneally with Rb_2 (body weight, 4.6 μmol/kg; n = 10) daily; and 3) OVX group, administered intraperitoneally with Rb_2 (body weight, 18.5 μmol/kg; n = 10) daily. Rb_2 was dissolved in distilled water. One week after the operation, the treatments commenced and continued for 12 weeks. Blood samples were obtained from the hearts in anesthetized mice and serum samples were prepared by centrifugation. The left femurs and 4th lumbar vertebrae (L4) of the mice were collected and the adherent tissue was discarded. All of the experimental procedures were officially approval by the Ethics in the Animal Research Committee of the Fourth Military Medical University (permission code 2010C00843).

Measurements of serum malondialdehyde (MDA) and reduced glutathione (GSH)

The activity of MDA in whole blood samples was determined using a lipid peroxidation MDA assay kit according to the manufacturer's instructions. The binding of thiobarbituric acid to malondialdehyde, which was formed during lipid peroxidation, results in a chromogenic complex. In the spectrophotometer, the change of absorption peak was detected at 532 nm. Colorimetry was used to detect the

Table 1
Real-time PCR primers for amplification of specific MC3T3-E1 mRNA.

Gene	Forward (5′–3′)	Reverse (5′–3′)
Alp	GCAGTATGAATTGAATCGGAACAAC	ATGGCCTGGTCCATCTCCAC
Colla1	GACATGTTCAGCTTTGTGGACCTC	GGGACCCTTAGGCCATTGTGTA
Ocn	ACCATCTTTCTGCTCACTCTGCT	CCTTATTGCCCTCCTGCTTG
Opn	TACGACCATGAGATTGGCAGTGA	TATAGGATCTGGGTGCAGGCTGTAA
β-Actin	CATCCGTAAAGACCTCTATGCCAAC	ATGGAGCCACCGATCCACA

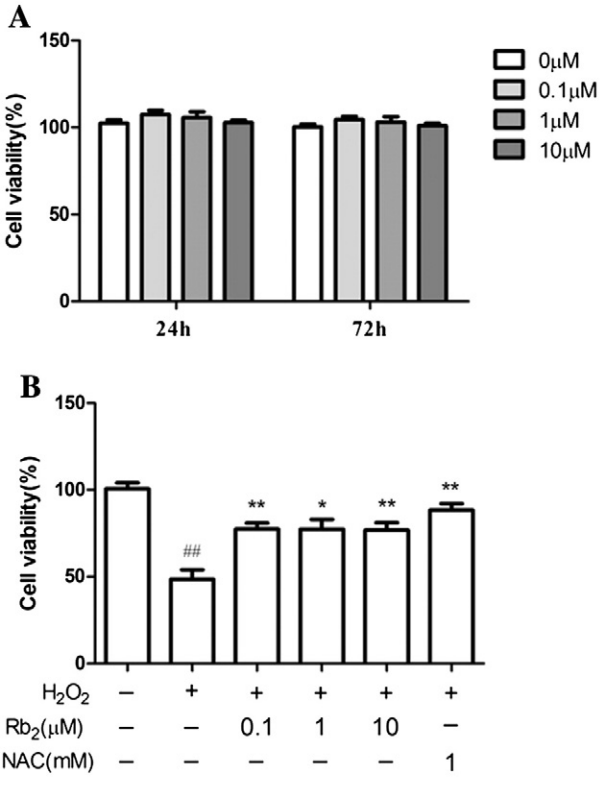

Fig. 2. Protection by Rb_2 on H_2O_2-induced cytotoxicity in MC3T3-E1 cells. A: MC3T3-E1 cells were cultured in different concentrations of Rb_2. B: MC3T3-E1 cells were administered with Rb_2 for 24 h before 0.3 mM H_2O_2 administration for 24 h. The control values for cell survival were 0.61 ± 0.02 OD. $^{\#\#}P < 0.01$ compared with untreated control cells; $^{*}P < 0.05$ and $^{**}P < 0.01$ in contrast to the group treated with H_2O_2 alone.

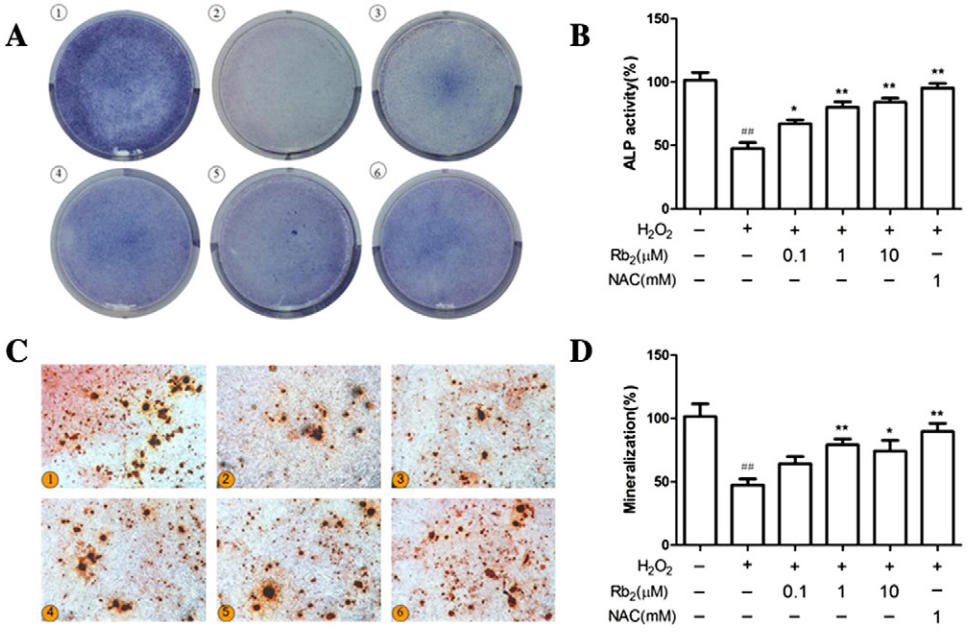

Fig. 3. Protection by Rb_2 on MC3T3-E1 cell dysfunction induced by H_2O_2. After induced for 6 days or 21 days, MC3T3-E1 cells were administered with Rb_2 for 24 h before 0.3 mM H_2O_2 administration for 24 h. A and B: Protection by Rb_2 on ALP staining and ALP activity in MC3T3-E1 cells after H_2O_2 treatment. The control value for ALP activity was 0.36 ± 0.03 unit/mg protein. C and D: Protective effects of Rb_2 on calcium deposition in MC3T3-E1 cells by Alizarin Red S staining after H_2O_2 treatment. The control values for mineralization were 0.73 ± 0.02 OD. ① Control group; ② H_2O_2; ③ H_2O_2 + Rb_2 (0.1 μM); ④ H_2O_2 + Rb_2 (1 μM); ⑤ H_2O_2 + Rb_2 (10 μM); ⑥ H_2O_2 + NAC (1 mM). $^{\#\#}P < 0.01$ compared with untreated control cells; $^{*}P < 0.05$ and $^{**}P < 0.01$ in contrast to the group treated with H_2O_2 alone.

malondialdehyde activity in the whole blood samples. Additionally, the activity of GSH was determined using the GSH assay kit. The GSH activity was determined by the reaction of GSH with 5.50-dithiobis-2-nitrobenzoic acid (DTNB) to produce a product that could be measured using a spectrophotometer at 412 nm.

Assessment of bone micro-architecture and bone mass by micro-computed tomography

The 4th lumbar vertebrae (L4) and the distal femur were scanned using explore Locus SP Pre-Clinical Specimen micro-CT (GE Healthcare,

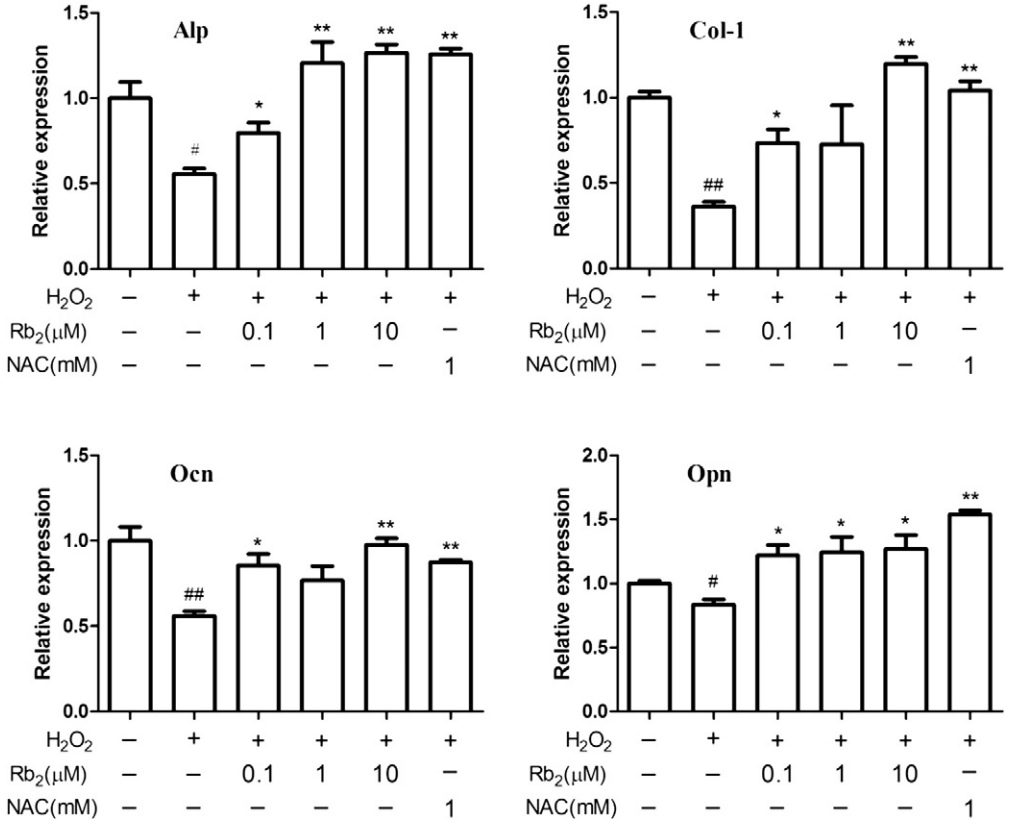

Fig. 4. Protection by Rb_2 on the transcriptional expressions of *Alp*, *Col1a1*, *Ocn* and *Opn* after H_2O_2 treatment. When induced for 6 days, MC3T3-E1 cells were administered with Rb_2 for 24 h before 0.3 mM H_2O_2 administration for 24 h. $^{\#}P < 0.05$ and $^{\#\#}P < 0.01$ compared with untreated control cells; $^{*}P < 0.05$ and $^{**}P < 0.01$ in contrast to the group treated with H_2O_2 alone.

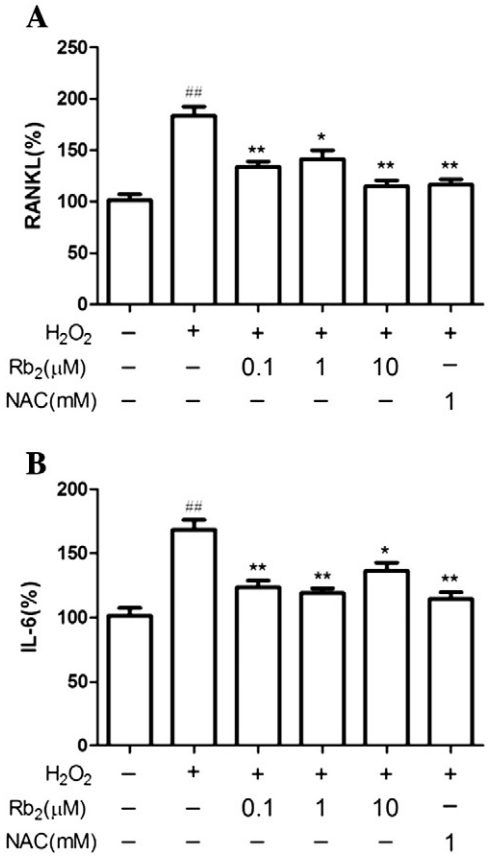

Fig. 5. Rb_2 inhibited the expressions of RANKL and IL-6 after H_2O_2 treatment. After osteogenic induction for 6 days, MC3T3-E1 cells were administered with Rb_2 for 24 h before 0.3 mM H_2O_2 administration for 24 h. A: Expression of RANKL with the presence of Rb_2 and/or H_2O_2. The control values for RANKL were 2.27 ± 0.18 ng/mg. B: Expression of IL-6 with the presence of Rb_2 and/or H_2O_2. The control values for IL-6 were 0.72 ± 0.17 ng/mg. $^{\#\#}P < 0.01$ compared with untreated control cells; $^{*}P < 0.05$ and $^{**}P < 0.01$ in contrast to the group treated with H_2O_2 alone.

USA) with 8-mm resolution, 50-kV tube voltage and 0.1-mA tube current. The reconstruction and 3D quantitative analyses were determined using software provided by a desktop micro-CT system (GE Healthcare, USA). Similar settings for scans and analyses were used for all of the samples. In the femur, the scanning regions were confined to the distal metaphysis, extending proximally 2.0 mm from the proximal tip of the primary spongiosa. The trabecular bone region from the vertebral body was outlined for each micro-CT slice, excluding both the cranial and caudal endplate regions. The following 3D indices in the defined region of interest (ROI) were analyzed: bone mineral density (BMD), connectivity density (Conn.D), structure model index (SMI), trabecular number (Tb.N), trabecular thickness (Tb.Th), trabecular separation (Tb.Sp) and relative bone volume over total volume (BV/TV, %). The operator who conducted the scan analysis was blinded to the procedure associated with the specimens.

Histological examination by Van Gieson (VG) staining

The 4th lumbar vertebrae and the left femur of all of the mice were collected and fixed in 4% paraformaldehyde for 48 h. After dehydration and embedding, the 4th lumbar vertebrae and the distal femur were embedded in polymethyl-methacrylate (PMMA) and processed into 240-mm-thick sections in the coronal plane using a rotation microtome. Subsequently, all of the sections were hand-grounded to a thickness of 20 mm for VG staining, which was used for staining collagen fiber [32].

Statistical analysis

The data represented the mean ± SD values of multiple repeats of the same experiment ($n = 5$). The data for all of the measurements were analyzed using a one-way analysis of variance (ANOVA) with subsequent post hoc multiple comparison by Dunnett's test. Statistically significant values were defined as $P < 0.05$.

Results

Rb_2 inhibited H_2O_2-induced cytotoxicity in MC3T3-E1 cells

Before the anti-cytotoxicity effect of Rb_2 was tested, the toxicity of Rb_2 on MC3T3-E1 was observed. The results showed that Rb_2 treatment alone did not affect cell survival at the consistencies tested in this experiment (Fig. 2A). Subsequently, we tested the survival of MC3T3-E1 cells to observe the defensive effects by Rb_2 on the repercussion of the cells after H_2O_2-induced oxidative damage. We implemented oxidative damage on MC3T3-E1 cells using 0.3 mM H_2O_2 for 24 h. When different concentrations of Rb_2 (0.1, 1, 10 μM) were administered to MC3T3-E1 cells for 24 h before H_2O_2 treatment, the viability of the cells increased compared to the group without Rb_2 treatment, which indicates that Rb_2, in part, inhibited H_2O_2-induced cytotoxicity (Fig. 2B). N-acetyl-L-cysteine represented the positive control, which significantly suppressed cytotoxicity induced by H_2O_2 at 1 mM.

Protection by Rb_2 on H_2O_2-induced dysfunction of MC3T3-E1 cells

We tested the protective effect of Rb_2 on H_2O_2-induced dysfunction of MC3T3-E1 cells by evaluating osteoblast differentiation and mineralization with ALP staining, ALP activity and Alizarin Red S staining. Additionally, we detected the expression of osteogenic genes including *Alp*, *Col1a1*, *Ocn* and *Opn*. Compared with the control group, all markers of osteogenic differentiation, such as ALP expression, calcium deposition and osteogenic genes (Figs. 3 and 4), decreased after treatment of H_2O_2. However, when we pretreated MC3T3-E1 cells with Rb_2 (0.1 μM, 1 μM, and 10 μM), cellular ALP expression (Fig. 3A) and activity (Fig. 3B) increased in a dose-dependent manner. As shown in Fig. 3C and D, Rb_2 (0.1 μM, 1 μM, and 10 μM) exhibited a good recovery effect on calcium deposition, which was suppressed by H_2O_2. Furthermore, pretreatment with Rb_2 partially elevated the expression of osteogenic genes compared with the group of H_2O_2 treated alone (Fig. 4). Our data indicated that Rb_2, in part, attenuated H_2O_2-induced dysfunction of MC3T3-E1 cells.

Rb_2 inhibited RANKL and IL-6 expression in MC3T3-E1 cells

Osteoblasts always express and secrete several cytokines, which bind to receptors in osteoclasts and affect osteoclast activity in bone remodeling. RANKL and IL-6 are two essential bone-resorbing factors expressed in osteoblasts. After the addition of 0.3 mM H_2O_2, the expressions of RANKL and IL-6 increased. However, when pretreated with Rb_2 of 0.1 μM, 1 μM and 10 μM, the elevated expressions of RANKL and IL-6 were, in part, inhibited (Fig. 5).

Rb_2 inhibited the production of reactive oxygen species induced by H_2O_2 in MC3T3-E1 cells

To clarify whether the cell-protective capacity of Rb_2 was associated with its antioxidant property, we tested ROS production using a fluorescent probe DCFH-DA. The results in Fig. 6 showed that when MC3T3-E1 cells were treated with 0.3 mM H_2O_2, ROS increased. These data indicated that H_2O_2 stimulated the generation of oxidants and resulted in oxidative stress to MC3T3-E1 cells. However, when pretreated with Rb_2 of different concentrations, ROS production was partially suppressed

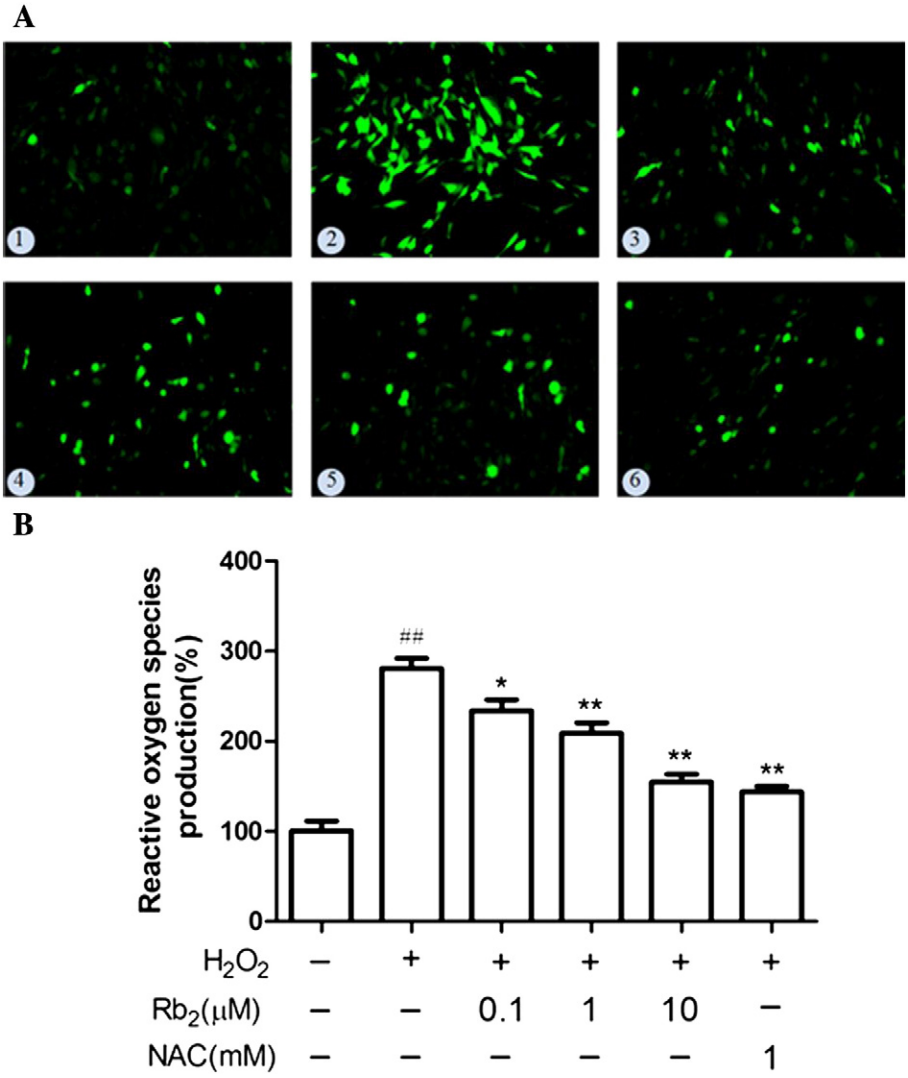

Fig. 6. Rb_2 inhibited H_2O_2-induced ROS expression in MC3T3-E1 cells. After osteogenic induction for 6 days, the cells were administered with Rb_2 for 24 h before a 0.3 mM H_2O_2 administration for 24 h. A: ROS detection by fluorescent probe DCFH-DA; B: quantitative analysis of ROS detection. ① Control group; ② H_2O_2; ③ H_2O_2 + Rb_2 (0.1 μM); ④ H_2O_2 + Rb_2 (1 μM); ⑤ H_2O_2 + Rb_2 (10 μM); ⑥ H_2O_2 + NAC (1 mM). $^{\#\#}P < 0.01$ compared with untreated control cells; $^{*}P < 0.05$ and $^{**}P < 0.01$ in contrast to the group treated with H_2O_2 alone.

(Fig. 6). These results suggested that the protection by Rb_2 might be related to its antioxidant activity.

Rb_2 inhibited serum oxidative damage of ovariectomized mice

To test whether Rb_2 can inhibit serum oxidative damage caused by estrogen insufficiency, the activities of serum malondialdehyde (MDA) and reduced glutathione (GSH) were observed in ovariectomized mice with or without Rb_2 intervention. The results in Fig. 7 showed that in contrast to the sham-operated group, the activity of MDA in serum increased, whereas the GSH activity in the ovariectomized group decreased. However, Rb_2 treatment partly rescued the serum activities of MDA and GSH.

Rb_2 improved bone mass and bone structure of ovariectomized mice

To evaluate Rb_2 acting on trabecular bone mass and micro-architecture, different concentrations of Rb_2 were supplemented to the ovariectomized (OVX) mice. When all of the mice were collected at 13 weeks after operation, there were no significant differences in body weights of all four groups. The body weights of the sham-operated group, OVX group, OVX + Rb_2 (4.6 μmol/kg) group and OVX + Rb_2 (18.5 μmol/kg) group were 24.26 ± 0.99 g, 24.12 ± 1.06 g, 24.03 ± 1.09 g and 24.07 ± 0.98 g, respectively. The micro-architectures of distal femurs are shown in Fig. 8A and B. The analyses of the trabecular bone of the 4th lumbar vertebrae (L4) and the distal femur showed that ovariectomy reduced bone mass and deteriorated bone micro-architecture, which was indicated through decreases in BMD, Conn.D, Tb.N, Tb.Th and BV/TV (Fig. 8C and D) ($P < 0.05$). SMI and Tb.Sp exhibited increases that contributed to ovariectomy ($P < 0.05$), as shown in Fig. 8E and F. However, the treatment of ovariectomized mice with 4.6 μmol/kg or 18.5 μmol/kg Rb_2, in part, rescued these bone parameters and improved the micro-architecture of the trabecular bone in the 4th lumbar vertebrae and the distal femur. Moreover, we evaluated the changes of bone micro-architecture by VG staining. As shown in Fig. 8G and H, compared with the sham-operated group, the number of trabeculae decreased and the trabecular space became broader in the OVX group. The supplement of Rb_2 reversed these changes by an elevated number of trabecular bone and a reduction of trabecular bone space (Fig. 8G and H). These results were consistent with the micro-CT data (Fig. 8A–F).

Discussion

The reactive oxygen species are highly reactive oxygen free radicals or non-radical molecules, which include hydrogen peroxide (H_2O_2),

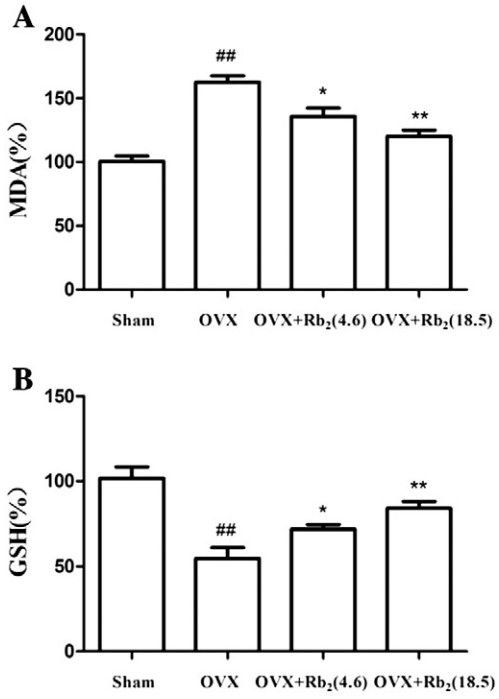

Fig. 7. Rb_2 inhibited serum oxidative damage in the ovariectomized model. A: Serum MDA concentrations in OVX mice that were administered different concentrations of Rb_2. B: Serum GSH concentrations in OVX mice that were administered different concentrations of Rb_2. Groups: Sham; OVX; OVX + Rb_2 (4.6 μmol/kg); OVX + Rb_2 (18.5 μmol/kg). The control values for MDA and GSH were 9.24 ± 0.67 nM/mg and 11.87 ± 1.27 nM/mg. $^{\#\#}P < 0.01$ compared with the sham group; $^{*}P < 0.05$ and $^{**}P < 0.01$ in contrast to the OVX group.

superoxide anion ($O_2^{\bullet -}$) and hydroxyl radical (•OH) [33]. Their overproduction induces oxidative stress. A considerable number of studies indicated that increased oxidative stress was involved in the pathogenesis of osteoporosis caused by estrogen deficiency and aging [34,35]. Because of good stability and property to pass through cell membranes, hydrogen peroxide is favorable to serve as both an extra- and an intercellular signal [36]. Therefore, an *in vitro* H_2O_2-induced oxidative damage model was used in this study. The study of Zhang et al. showed that the treatment of 0.3 mM H_2O_2 for 24 h reduced the number of MC3T3-E1 cells to 50% and that 0.3 mM H_2O_2 was suitable for generating an *in vitro* oxidative stress model [32]. Therefore, we used 0.3 mM H_2O_2 for 24 h to make an oxidative damage model in the present study. Our data showed that H_2O_2 toxicity was reversed to a certain degree by pretreatment with Rb_2. This study demonstrated that Rb_2, in part, decreased H_2O_2-induced cytotoxicity on MC3T3-E1 cells.

Oxidative damage not only affects osteoblast survival but also has an impact on its differentiation. H_2O_2-induced oxidative damage is reported to inhibit osteoblast differentiation in primary murine bone marrow stem cells and to reduce the expression of osteoblast markers in osteoblastic MC3T3-E1 cells [19,37]. Our study also showed that H_2O_2 supplement was linked to a reduction of cellular alkaline phosphatase activity, a decrease of calcium mineralization and lowered expressions of osteogenic genes, including *Alp*, *Col1a1*, *Ocn* and *Opn*, which confirms previous results that cytotoxicity of H_2O_2, in part, results in MC3T3-E1 cell dysfunction. Moreover, our data showed that H_2O_2-induced inhibition of osteogenic differentiation could be reversed by Rb_2. Rb_2 alone could not significantly enhance MC3T3-E1 cell survival and osteogenic differentiation within experimented consistencies. Therefore, we speculated that the antioxidant property of Rb_2 contributed to the protective effect. Because Rb_2 improves osteoblastic survival and differentiation against oxidative damage, Rb_2 might become an anti-osteoporosis agent in the bone metabolism area.

Several pathways and cytokines couple the link between osteoblasts and osteoclasts. RANKL and IL-6 are generated by osteoblasts and function as bone-resorbing cytokines by stimulating osteoclast activity. RANKL belongs to the superfamily of tumor necrosis factor [38]. By binding to RANK, RANKL leads to osteoclastic differentiation, prolongs osteoclastic activity and increases bone resorption [11]. Several studies have shown that reactive oxygen species could elevate the expression of RANKL in osteoblasts [39]. IL-6 is also generated by osteoblasts when it is motivated by IL-1, TNF-α, and lipopolysaccharide [40]. IL-6 could affect the expression of RANKL, improve osteoclast development and be a significant pathogenic factor of estrogen deficiency osteoporosis [41,42]. It was reported that reactive oxygen species might indirectly influence osteoclasts by increasing the expression of bone-resorptive cytokines, which are highly involved in estrogen deficiency osteoporosis [43]. In our study, Rb_2 was noted to inhibit, in part, the H_2O_2-induced generations of RANKL and IL-6 in MC3T3-E1 cells. The reductions of RANKL and IL-6 might contribute to the anti-resorbing property, which Rb_2 exhibited.

Ginsenoside-Rb_2 (Rb_2), which is extracted from *Panax ginseng*, belongs to traditional Chinese medicine. Recently, its anti-oxidative property has been reported [16]. In this study, we could reverse, in part, H_2O_2-induced production of reactive oxygen species by pretreatment with Rb_2 for 24 h. Our data indicated that Rb_2 might be a useful antioxidant to protect MC3T3-E1 cells from cytotoxicity induced by oxidative damage. Consequently, the protection by Rb_2 to MC3T3-E1 cells could be mediated *via* its antioxidant property. The beneficial effect of Rb_2 might be linked to reduced oxidative damage and bone-resorbing cytokines. However, the molecular mechanism has not been established. Compared with other growth factors, reactive oxygen species result in the retention of FoxOs in the nucleus and the activation of their transcription [44]. FoxO protein family is characterized by a common winged-helix DNA binding domain called Forkhead box [45]. Animal studies have demonstrated that in response to oxidative damage, c-jun kinase (JNK) and mammalian sterile 20-related kinase-1 (Mst1) bond and phosphorylate FoxOs in a direct manner [46–49]. FoxO-dependent oxidative defense systems provide an approach for dealing with oxygen free radicals that are constantly produced by the aerobic metabolism of osteoblasts and are therefore essential for bone mass balance [50]. Under these circumstances, we deduced that Rb_2 provided protective effects against cytotoxicity and osteoblast dysfunction induced by H_2O_2 through the JNK, Mst1 and FoxOs signaling pathway. In additional studies, we will explore this molecular mechanism.

The mechanism by which estrogen deficiency activates bone loss has not been established. Recently, oxidative damage has been documented to result in postmenopausal osteoporosis. Almeida et al. reported that similar increases in oxidative stress and $p66^{shc}$ phosphorylation observed with age-related changes in bone of C57BL/6 mice were caused by removing gonads in the female or male mice [17,20]. Moreover, the alterations were ameliorated by administering antioxidants, such as N-acetyl-L-cysteine, ascorbate, and catalase, which is as effective as hormone replacement [9]. Malondialdehyde (MDA), which commonly served as a trustful parameter in evaluating the oxidative damage status [51], is an end product of lipid peroxidation induced by reactive oxygen species. Reduced glutathione (GSH) is an intracellular antioxidant, which prevents cells from oxidative stress caused by free radicals, peroxides and toxins. It can effectively remove $O_2^{\bullet -}$ and provide electrons for glutathione peroxidase to transform H_2O_2 into H_2O [52]. Additionally, GSH reduction is a marker of oxidative damage [53]. Our research showed that Rb_2 administration for 12 weeks reversed, in part, serum MDA and GSH activities of ovariectomized mice.

Sharing similarities with postmenopausal women, ovariectomized mice experience significant bone loss due to estrogen deficiency, which primarily results from trabecular bone loss [54]. Therefore, the trabecular bone micro-architecture is considered to be a proper predictor of OVX-induced bone loss and bone quality deterioration [55]. The micro-architecture of trabecular bone has been shown to

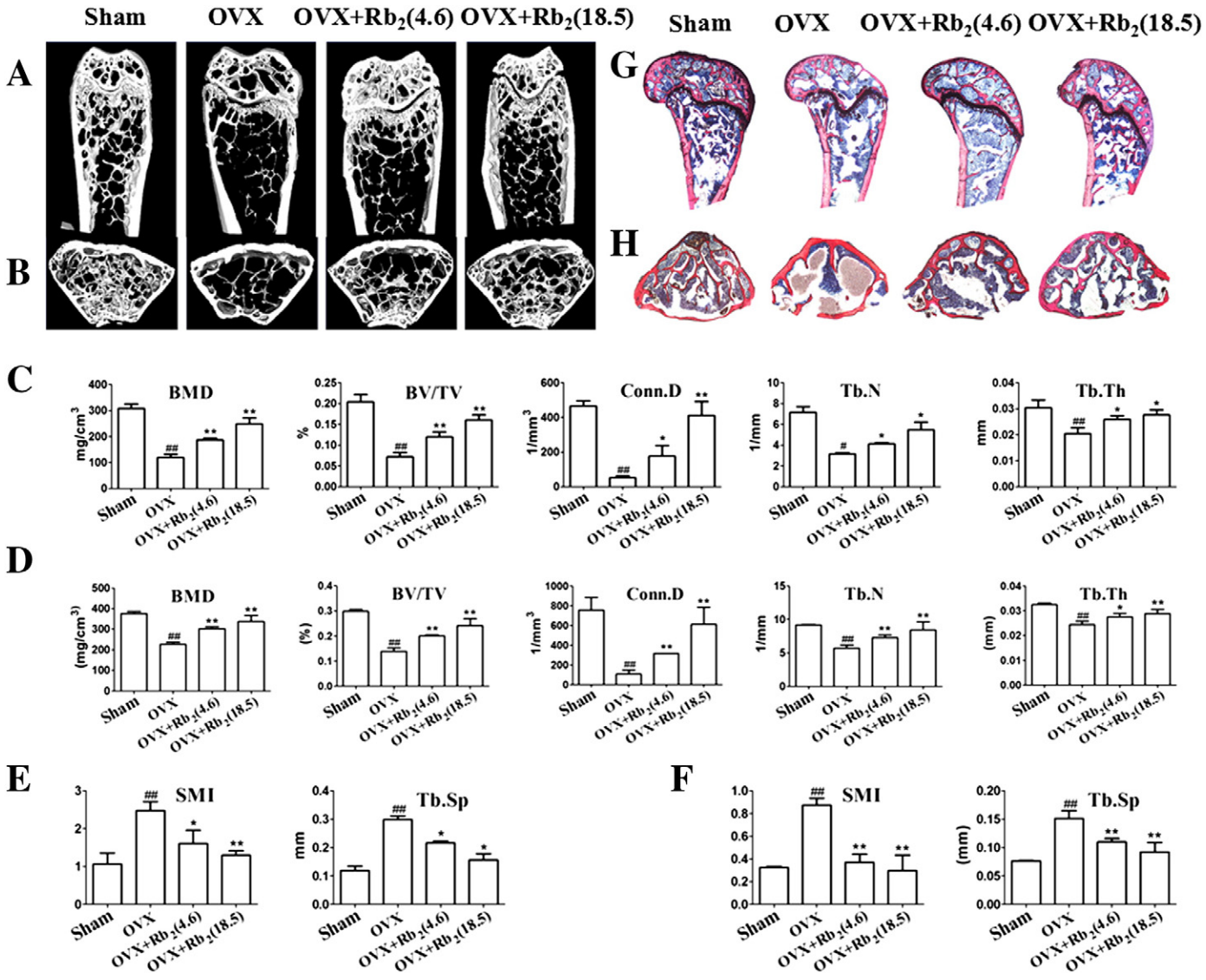

Fig. 8. Protection by Rb_2 on the bone mass and micro-architecture of trabecular bone of OVX mice. A and B: Analysis of micro-CT in the distal metaphyseal femur region. Groups: Sham; OVX; OVX + Rb_2 (4.6 μmol/kg); OVX + Rb_2 (18.5 μmol/kg). C and E: Analysis of micro-CT quantification in the distal metaphyseal femur region. D and F: Analysis of micro-CT quantification in the 4th lumbar vertebrae. The following 3D indices in the defined region of interest (ROI) were analyzed: BMD, Conn.D, SMI, Tb.N, Tb.Th, Tb.Sp and BV/TV. G and H: Van Gieson (VG) staining of the distal femur and body of the 4th lumbar vertebrae. The figure was 40× and 100× of the original section. *P < 0.05 and ##P < 0.01 compared with the sham group; *P < 0.05 and **P < 0.01 in contrast to the OVX group.

dramatically deteriorate after ovariectomy by both micro-CT scanning and VG staining [32,56]. Nevertheless, these negative effects could be reversed, to some degree, after administering Rb_2. These results further confirmed that Rb_2 might, in part, ameliorate trabecular micro-architecture and bone mass of OVX mice and that Rb_2 might be a good candidate for the prevention and the treatment of estrogen-deficient osteoporosis.

To conclude, the results described in this article indicated that in an *in vitro* analysis, ginsenoside-Rb_2 protected osteoblastic MC3T3-E1 cells from cytotoxicity and osteoblast dysfunction induced by hydrogen peroxide at 0.1 to 10 μM. This activity is linked to a reduction of oxidative damage and bone-resorbing cytokines. More importantly, ginsenoside-Rb_2 decreased serum reactive oxygen species to a certain degree and partly reversed estrogen-deficient effects *in vivo* at doses of 4 to 18 μmol/kg body weight. Ginsenoside-Rb_2 may act as a substantive alternative in bone metabolic diseases, especially osteoporosis. Extensive research is needed in the future to explore the intricate molecular mechanisms of ginsenoside-Rb_2 on bone metabolism.

Acknowledgments

This work was supported by the Ministry of Science and Technology of the People's Republic of China (2011CB964703), National High Technology Research and Development Program 863 (2012AA020502) and National Natural Science Foundation of China (30901504), and the Program for Changjiang Scholars and Innovative Research Team in University (no. IRT1053). No benefits in any form have been or will be received from a commercial party directly or indirectly by the authors of this manuscript.

References

[1] Sanchez-Rodriguez MA, Ruiz-Ramos M, Correa-Munoz E, Mendoza-Nunez VM. Oxidative stress as a risk factor for osteoporosis in elderly Mexicans as characterized by antioxidant enzymes. BMC Musculoskelet Disord 2007;8:124.
[2] Bouillon, Burckhardt R, Christiansen P, Fleisch C, Fujita HA, Gennari T, et al. Consensus development conference: diagnosis, prophylaxis and treatment of osteoporosis. Am J Med 1993;94:646–50.

[3] Sendur OF, Turan Y, Tastaban E, Serter M. Antioxidant status in patients with osteoporosis: a controlled study. Joint Bone Spine 2009;76:514–8.
[4] Witko-Sarsat V, Friedlander M, Capeillere-Blandin C, Nguyen-Khoa T, Nguyen AT, Zingraff J, et al. Advanced oxidation protein products as a novel marker of oxidative stress in uremia. Kidney Int 1996;49:1304.
[5] Ozgocmen S, Kaya H, Fadillioglu E, Aydogan R, Yilmaz Z. Role of antioxidant systems, lipid peroxidation, and nitric oxide in postmenopausal osteoporosis. Mol Cell Biochem 2007;295:45–52.
[6] Ozgocmen S, Kaya H, Fadillioglu E, Yilmaz Z. Effects of calcitonin, risedronate, and raloxifene on erythrocyte antioxidant enzyme activity, lipid peroxidation, and nitric oxide in postmenopausal osteoporosis. Arch Med Res 2007;38:196–205.
[7] Muthusami S, Ramachandran I, Muthusamy B, Vasudevan G, Prabhu V, Subramaniam V, et al. Ovariectomy induces oxidative stress and impairs bone antioxidant system in adult rats. Clin Chim Acta 2005;360:81–6.
[8] Linnane AW, Eastwood H. Cellular redox regulation and prooxidant signaling systems: a new perspective on the free radical theory of aging. Ann N Y Acad Sci 2006;1067:47.
[9] Manolagas SC. From estrogen-centric to aging and oxidative stress: a revised perspective of the pathogenesis of osteoporosis. Endocr Rev 2010;31:266–300.
[10] Theill LE, Boyle WJ, Penninger JM. RANK-L and RANK: T cells, bone loss, and mammalian evolution. Annu Rev Immunol 2002;20:795–823.
[11] Boyle WJ, Simonet WS, Lacey DL. Osteoclast differentiation and activation. Nature 2003;423:337–42.
[12] Karsenty G, Wagner EF. Reaching a genetic and molecular understanding of skeletal development. Dev Cell 2002;2:389–406.
[13] Soltanoff CS, Yang S, Chen W, Li YP. Signaling networks that control the lineage commitment and differentiation of bone cells. Crit Rev Eukaryot Gene Expr 2009;19:1–46.
[14] Huang W, Yang S, Shao J, Li YP. Signaling and transcriptional regulation in osteoblast commitment and differentiation. Front Biosci 2007;12:3068–92.
[15] Isomura H, Fujie K, Shibata K, Inoue N, Iizuka T, Takebe G, et al. Bone metabolism and oxidative stress in postmenopausal rats with iron overload. Toxicology 2004; 197:93–100.
[16] Lee NK, Choi YG, Baik JY, Han SY, Jeong DW, Bae YS, et al. A crucial role for reactive oxygen species in RANKL-induced osteoclast differentiation. Blood 2005;106:852–9.
[17] Lean JM, Davies JT, Fuller K, Jagger CJ, Kirstein B, et al. A crucial role for thiol antioxidants in estrogen-deficiency bone loss. J Clin Invest 2003;112:915–23.
[18] Lean JM, Jagger CJ, Kirstein B, Fuller K, Chambers TJ. Hydrogen peroxide is essential for estrogen-deficiency bone loss and osteoclast formation. Endocrinology 2005; 146:728–35.
[19] Arai M, Shibata Y, Pugdee K, Abiko Y, Ogata Y. Effects of reactive oxygen species (ROS) on antioxidant system and osteoblastic differentiation in MC3T3-E1 cells. IUBMB Life 2007;59:27–33.
[20] Almeida M, Han L, Martin-Millan M, Plotkin LI, Stewart SA, Roberson PK, et al. Skeletal involution by age-associated oxidative stress and its acceleration by loss of sex steroids. J Biol Chem 2007;282:27285–97.
[21] Jilka RL, Almeida M, Ambrogini E, Han L, Roberson PK, et al. Decreased oxidative stress and greater bone anabolism in the aged, as compared to the young, murine skeleton by parathyroid hormone. Aging Cell 2010;9:851–67.
[22] Ma WG, Mizutani M, Malterud KE, Lu SL, Ducrey B, Tahara S. Saponins from the roots of *Panax notoginseng*. Phytochemistry 1999;52:1133–9.
[23] Lee KT, Jung TW, Lee HJ, Kim SG, Shin YS, Whang WK. The antidiabetic effect of ginsenoside Rb_2 via activation of AMPK. Arch Pharm Res 2011;34(7):1201–8.
[24] Kim EJ, Lee HI, Chung KJ, Noh YH, Ro Y, Koo JH. The ginsenoside-Rb_2 lowers cholesterol and triacylglycerol levels in 3T3-L1 adipocytes cultured under high cholesterol or fatty acids conditions. BMB Rep 2009;42(4):194–9.
[25] Fujimoto J, Sakaguchi H, Aoki I, Toyoki H, Khatun S, Tamaya T. Inhibitory effect of ginsenoside-Rb_2 on invasiveness of uterine endometrial cancer cells to the basement membrane. Eur J Gynaecol Oncol 2001;22(5):339–41.
[26] Kang KS, Kim HY, Baek SH, Yoo HH, Park JH, Yokozawa T. Study on the hydroxyl radical scavenging activity changes of ginseng and ginsenoside-Rb_2 by heat processing. Biol Pharm Bull 2007;30(4):724–8.
[27] Kang KS, Kang BC, Lee BJ, Che JH, Li GX, Trosko JE, et al. Preventive effect of epicatechin and ginsenoside Rb_2 on the inhibition of gap junctional intercellular communication by TPA and H_2O_2. Cancer Lett 2000;152:97–106.
[28] Kim YH, Park KH, Rho HM. Transcriptional activation of the Cu, Zn-superoxide dismutase gene through the AP2 site by ginsenoside Rb_2 extracted from a medicinal plant, *Panax ginseng*. J Biol Chem 1996;40:24539–43.
[29] Li Y, Tang L, Duan Y, Ding Y. Up-regulation of MMP-13 and TIMP-1 expression in response to mechanical strain in MC3T3-E1 osteoblastic cells. BMC Res Notes 2010;3:309.
[30] Li Y, Ma W, Feng Z, Wang Z, Zha N, Deng B, et al. Effects of irradiation on osteoblast-like cells on different titanium surfaces in vitro. J Biomed Mater Res B Appl Biomater 2012;101B:9–17.
[31] Boyd Steven K, Davison Peter, Müller Ralph, Gasser Jürg A. Monitoring individual morphological changes over time in ovariectomized rats by in vivo micro-computed tomography. Bone 2006;39:854–62.
[32] Zhang JK, Yang L, Meng GL, Yuan Z, Fan J, Li D, et al. Protection by salidroside against bone loss via inhibition of oxidative stress and bone-resorbing mediators. PLoS ONE 2013;8(2):e57251.
[33] Shi Y, Tang B, Yu PW, Tang B, Hao YX, Lei X, et al. Autophagy protects against oxaliplatin-induced cell death via ER stress and ROS in Caco-2 cells. PLoS ONE 2012;7:e51076.
[34] Baek KH, Oh KW, Lee WY, Lee SS, Kim MK, Kwon HS, et al. Association of oxidative stress with postmenopausal osteoporosis and the effects of hydrogen peroxide on osteoclast formation in human bone marrow cell cultures. Calcif Tissue Int 2010;87:226–35.
[35] Maggio D, Barabani M, Pierandrei M, Polidori MC, Catani M, Catani M, et al. Marked decrease in plasma antioxidants in aged osteoporotic women: results of a cross-sectional study. J Clin Endocrinol Metab 2003;88:1523–7.
[36] Denisova NA, Cantuti-Castelvetri I, Hassan WN, Paulson KE, Joseph JA. Role of membrane lipids in regulation of vulnerability to oxidative stress in PC12 cells: implication for aging. Free Radic Biol Med 2001;30:671–8.
[37] Liu AL, Zhang ZM, Zhu BF, Liao ZH, Liu Z. Metallothionein protects bone marrow stromal cells against hydrogen peroxide-induced inhibition of osteoblastic differentiation. Cell Biol Int 2004;28:905–11.
[38] Lacey DL, Timms E, Tan HL, Kelley MJ, Dunstan CR, Burgess T, et al. Osteoprotegerin ligand is a cytokine that regulates osteoclast differentiation and activation. Cell 1998;93:165–76.
[39] Bai XC, Lu D, Liu AL, Zhang ZM, Li XM, Zou ZP, et al. Reactive oxygen species stimulates receptor activator of NF-kappaB ligand expression in osteoblast. J Biol Chem 2005;280:17497–506.
[40] Girasole G, Jilka RL, Passeri G, Boswell S, Boder G, Williams DC, et al. 17 beta-estradiol inhibits interleukin-6 production by bone marrow-derived stromal cells and osteoblasts in vitro: a potential mechanism for the antiosteoporotic effect of estrogens. J Clin Invest 1992;89:883–91.
[41] Kurihara N, Bertolini D, Suda T, Akiyama Y, Roodman GD. IL-6 stimulates osteoclast-like multinucleated cell formation in long term human marrow cultures by inducing IL-1 release. J Immunol 1990;144:4226–30.
[42] Papanicolaou DA, Vgontzas AN. Interleukin-6: the endocrine cytokine. J Clin Endocrinol Metab 2000;85:1331–3.
[43] Kitazawa R, Kimble RB, Vannice JL, Kung VT, Pacifici R. Interleukin-1 receptor antagonist and tumor necrosis factor binding protein decrease osteoclast formation and bone resorption in ovariectomized mice. J Clin Invest 1994;94:2397–406.
[44] Van der HA, Burgering BM. Stressing the role of FoxO proteins in lifespan and disease. Nat Rev Mol Cell Biol 2007;8:440–50.
[45] Greer EL, Brunet A. FOXO transcription factors at the interface between longevity and tumor suppression. Oncogene 2005;24:7410–25.
[46] Essers MA, Weijzen S, Vries-Smits AM, Saarloos I, de Ruiter ND, Bos JL, et al. FOXO transcription factor activation by oxidative stress mediated by the small GTPase Ral and JNK. EMBO J 2004;23:4802–12.
[47] Lehtinen MK, Yuan Z, Boag PR, Yang Y, Villen J, Becker EB, et al. A conserved MST-FOXO signaling pathway mediates oxidative-stress responses and extends life span. Cell 2006;125:987–1001.
[48] Wang MC, Bohmann D, Jasper H. JNK extends life span and limits growth by antagonizing cellular and organism-wide responses to insulin signaling. Cell 2005;121:115–25.
[49] Oh SW, Mukhopadhyay A, Svrzikapa N, Jiang F, Davis RJ, Tissenbaum HA. JNK regulates lifespan in *Caenorhabditis elegans* by modulating nuclear translocation of forkhead transcription factor/DAF-16. Proc Natl Acad Sci U S A 2005;102:4494–9.
[50] Ambrogini E, Almeida M, Martin-Millan M, Paik JH, DePinho RA, Han L, et al. FoxO-mediated defense against oxidative stress in osteoblasts is indispensable for skeletal homeostasis in mice. Cell Metab 2010;11(2):136.
[51] Cakatay U, Aydin S, Yanar K, Uzun H. Gender-dependent variations in systemic biomarkers of oxidative protein, DNA, and lipid damage in aged rats. Aging Male 2010;13:51.
[52] Estrela JM, Ortega A, Obrador E. Glutathione in cancer biology and therapy. Crit Rev Clin Lab Sci 2006;43:143–81.
[53] Kinov P, Leithner A, Radl R, Bodo K, Khoschsorur GA, Schauenstein K, et al. Role of free radicals in aseptic loosening of hip arthroplasty. J Orthop Res 2006;24:55–62.
[54] Kim TH, Jung JW, Ha BG, Hong JM, Park EK, Kim HJ, et al. The effects of luteolin on osteoclast differentiation, function in vitro and ovariectomy-induced bone loss. J Nutr Biochem 2011;22:8–15.
[55] Chappard D, Basle MF, Legrand E, Audran M. Trabecular bone microarchitecture: a review. Morphologie 2008;92:162–70.
[56] Campbell GM, Buie HR, Boyd SK. Signs of irreversible architectural changes occur early in the development of experimental osteoporosis as assessed by in vivo micro-CT. Osteoporos Int 2008;19:1409–19.